Towards Selective Delivery of a Ruthenium(II) Polypyridyl Complex-Containing Bombesin Conjugate into Cancer Cells

Maria José Silva, Robin Vinck, Youchao Wang, Bruno Saubaméa, Mickaël Tharaud, Elena Dominguez-Jurado, Johannes Karges, Pedro M P Gois, Gilles Gasser

Towards Selective Delivery of a Ruthenium(II) Polypyridyl Complex-Containing Bombesin Conjugate into Cancer Cells

Maria J. S. A. Silva,[a,b] Robin Vinck,[b] Youchao Wang,[b] Bruno Saubaméa,[c] Mickaël Tharaud,[d] Elena Dominguez-Jurado,[e] Johannes Karges,[b] Pedro M. P. Gois[a]* and Gilles Gasser[b]*

[a] Research Institute for Medicines (iMed.ULisboa), Faculty of Pharmacy, Universidade de Lisboa, Lisbon, Portugal.

[b] Chimie ParisTech, PSL University, CNRS, Institute of Chemistry for Life and Health Sciences, Laboratory for Inorganic Chemical Biology, F-75005 Paris, France.

[c] Cellular and Molecular Imaging Facility, US25 Inserm, UAR3612 CNRS, Faculté de Pharmacie de Paris, Université Paris Cité, F-75006 Paris, France.

[d] Université Paris Cité, Institut de Physique du Globe de Paris, CNRS, F-75005 Paris, France.

[e] Faculty of Pharmacy of Albacete, Universidad de Castilla-La Mancha, 02008 Albacete, Spain.

* Corresponding authors: gilles.gasser@chimieparistech.psl.eu; WWW: www.gassergroup.com; Tel. +33 1 85 78 41 51; pedrogois@ff.ulisboa.pt; WWW: https://sites.ff.ulisboa.pt/goislab/; Tel. +351 217 946 400 (Ext. 14614)

ORCID-ID:

Dr. Maria J. S. A. Silva 0000-0003-4178-1942

Dr.Robin Vinck: 0000-0002-2730-0121

Youchao Wang: 0000-0002-7552-9334

Dr. Bruno Saubaméa: 0000-0002-6218-0460

Dr. Mickael Tharaud: 0000-0001-6131-655X

Elena Domínguez Jurado: 0000-0003-4235-7561

Dr. Johannes Karges: 0000-0001-5258-0260

Prof. Dr. Pedro M. P. Gois: 0000-0002-7698-630X

Prof. Dr. Gilles Gasser: 0000-0002-4244-5097

Abstract

There is an increasing number of novel Ru(II) polypyridyl complexes successfully applied as photosensitizers (PSs) for photodynamic therapy (PDT). Despite recent advances on optimized PSs with refined photophysical properties, the lack of tumoral selectivity is often a major hurdle for their clinical development. Herein, classical maleimide and versatile NHS-activated acrylamide strategies were employed to site-selectively conjugate a promising Ru(II) polypyridyl complex to the *N*-terminal Cys modified Bombesin (BBN) targeting unit. Surprisingly, the decreased cell uptake of these novel Ru-BBN conjugates in cancer cells did not hamper the high phototoxic activity of the Ru-containing bioconjugates and even decrease the toxicity of the constructs in the absence of light irradiation. Overall, while deceiving in terms of selectivity, our new bioconjugates could be still useful for advanced cancer treatment due to their non-toxicity in the dark.

Introduction

Photodynamic therapy (PDT) is a clinically approved technique that uses a photosensitizer (PS), light and endogenous molecular oxygen to generate toxic reactive oxygen species (ROS) such as singlet oxygen. In PDT, the spatiotemporal overlap of these three components and the limited radius of action of the generated ROS offers a uniquely selective method to target cancer cells.[1] Therefore, the discovery and development of new PSs, with extended lifetimes in the triplet state and high selectivity for cancer cells is highly desirable.[2]

The use of transition metal (TM) complexes for the detection and treatment of various diseases witnessed an impressive growth over the last decades,[3] and in PDT, the incorporation of TM enabled the design of a new class of advanced PSs.[4] Compared to purely organic PSs, the superior photophysical and photochemical performances of these complexes enable very efficient photocatalysis with much lower PS concentrations.[4b] Among the increasing number of TM-based PSs, Ru(II) polypyridyl complexes have been the most widely explored for PDT applications and diagnostics.[5] [Ru-(bathophenantroline)2(4,4′-dimethyl-2,2′-bipyridine)]$^{2+}$ (complex **[Ru-(bphen)$_2$(dmbipy)]$^{2+}$**, Figure 1) was reported by our group for PDT as this complex showed to have excited states lifetime within the nanoscale range and high singlet oxygen quantum yield.[6] Furthermore, this Ru(II) complex also demonstrated a high stability in DMSO and human plasma and negligible photobleaching upon light exposure. Additionally, this complex showed an impressive phototoxicity in the low micro- to nanomolar range upon irradiation at high wavelenghts (595 nm) in different cancer cell lines. However, it also displayed high cytotoxicity towards healthy cells even in the absence of light irradiation resulting in undesirable off-target

activity. Therefore, to take advantage of the PDT potential of this complex, it is vital to improve its selectivity to cancer cells while decreasing general cytotoxicity in the dark, for instance by incorporation a targeting unit to its structure.

Many efforts have been pursued to enhance tumor selectivity and cellular uptake of PSs either through active and passive targeting strategies.[7] Among them, bombesin peptide (BBN), and human gastrin releasing peptide (GRP), sharing the same *C*-terminal sequence of seven amino acids and a high affinity for the gastrin releasing peptide receptor (GRPR), have been extensively explored.[8] Both peptides exert similar physiopathological roles, including calcium mobilization, which is important for smooth muscle cells contraction, neurological functions as well as autocrine processes and hormone release in pancreatic, gastric, and endocrine systems.[9] More importantly, GRPR and GRP promote survival mechanisms in cancer cells and have been described to be overexpressed in many human tumors including nerve tissues, breast, small cell lung, gastric, pancreatic, colon, renal, cervical, prostate.[10] In fact, GRPR are one of the most frequently overexpressed classes of G protein-coupled receptors in those malignancies, which offers a great potential for therapeutic interventions.[9b] In general, GRPR agonists are rapidly taken up following their binding to GRPR receptors. This enables the selective and high accumulation of conjugated BBN-like analogs inside tumor cells overexpressing GRPR receptors.[11] According to recent studies, the conserved *C*-terminal sequence of BBN is of key importance to ensure its high binding affinity towards GRPR and promote the efficient internalization of truncated BBN peptides.[12] Thus, the *N*-terminal sequence is suitable for functionalization with fluorescent probes or active drugs without compromising the cellular uptake efficiency of BBN conjugates.[13] We also note that other metal complexes were coupled to bombesin derivatives, with more or less success in targeting abilities.[14]

Inspired by these seminal findings, herein we purposed the conjugation of an analog of $[Ru(bphen)_2(dmbipy)]^{2+}$ complex with the Bombesin peptide bearing a *N*-terminal Cys through the straightforward NHS-activated acrylamide and maleimide bioconjugation strategies.[15] The BBN peptide was explored as a Trojan Horse to enhance the selective delivery and accumulation this promising PDT agent in GRPR overexpressing cancerous cells.

Results and Discussion

As previously reported, functionalized NHS-activated acrylamides can be synthesized by reacting the di-NHS activated fumarate with the desired amine-containing payload in organic solvent at room temperature. To successfully employ this straightforward strategy for the synthesis of a Ru-complex NHS-activated acrylamide, a Ru(II) polypyridyl complex similar to

model complex **[Ru-(bphen)$_2$(dmbipy)]$^{2+}$** bearing a nucleophilic amine was prepared (see Supporting Information). First, commercially available $RuCl_3(H_2O)_3$ was converted into $RuCl_2(DMSO)_4$[16] for easier complexation with bathophenantroline (bphen) ligands under reflux conditions, to provide $Ru(bphen)_2Cl_2$.[17] The non-symmetric (4'-methyl-[2,2'-bipyridin]-4-yl)methanamine (dmbipyNH_2) ligand was obtained through Delépine amine synthesis from the 4-bromomethyl monosubstituted bipyridine.[18] Afterwards, $Ru(bphen)_2Cl_2$ complex and dmbipyNH_2 ligand were refluxed to provide the desired amine functionalized **[Ru(bphen)$_2$dmbipyNH$_2$](PF$_6$)$_2$** complex (**Ru-NH$_2$**). Finally, **Ru NHS-activated acrylamide** was prepared by mono-amidation of di-NHS activated fumarate (Scheme 1A) in acetonitrile at room temperature and fully characterized.

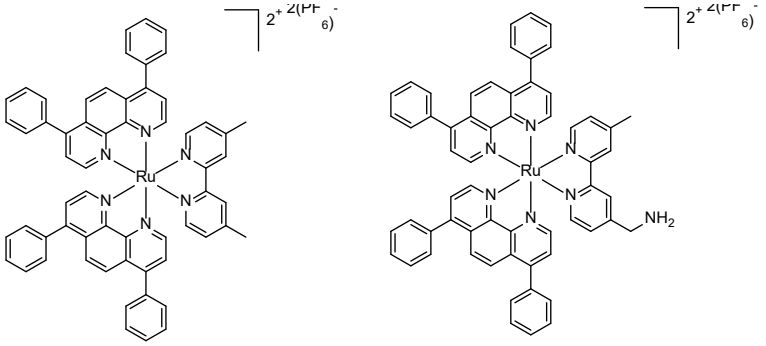

Figure 1. Structures of **[Ru-(bphen)$_2$(dmbipy)]$^{2+}$** and **Ru-NH$_2$** complexes.

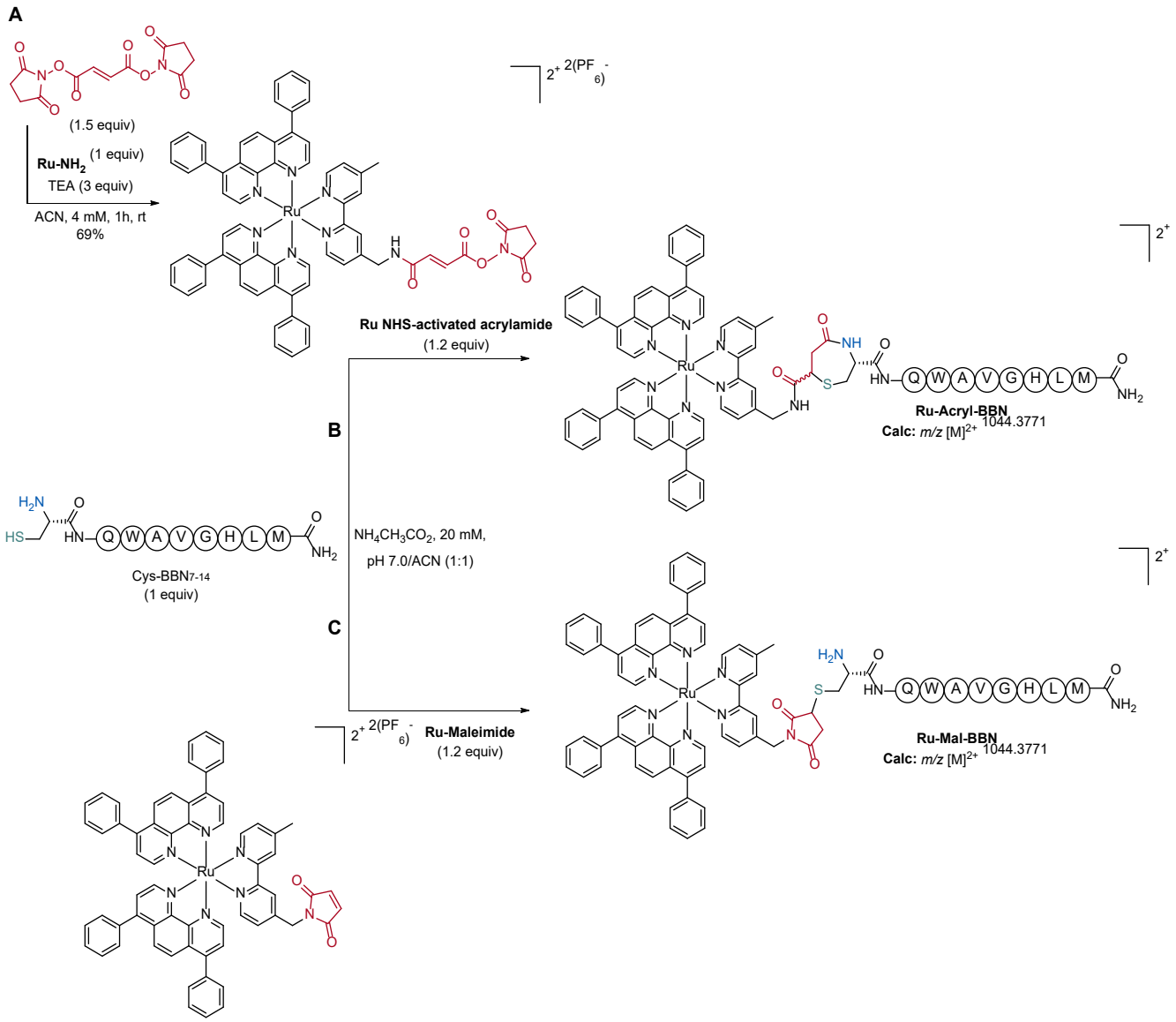

Scheme 1. **A**) Synthesis of **Ru NHS-activated acrylamide**. **B** and **C**) Bioconjugation reaction of Cys-BBN$_{7-14}$ with Ru NHS-activated acrylamide and Ru-Maleimide to afford bioconjugates **Ru-Acryl-BBN** and **Ru-Mal-BBN**, respectively.

Next, the bioconjugates **Ru-Acryl-BBN** (Scheme 1B) and the thiosuccinimide analog **Ru-Mal-BBN** (Scheme 1C) were prepared under mild conditions and in high purity according to HPLC and ESI$^+$-HRMS analysis. The photophysical characterization of both **Ru-Acryl-BBN** and **Ru-NH$_2$** show a bipyridine centered transitions absorption in the UV region (280 nm) and a typical metal to ligand charge transfer (MLCT) absorption in the visible region (Figure 2). To better understand the photophysical properties, photostability experiments were performed to **Ru-NH$_2$** in PBS and Acetonitrile. As shown in Figure 3, **Ru-NH$_2$** was relatively stable within 10 minutes of irradiation, after that a general decrease in absorbance was observed in acetonitrile and PBS, which could

be attributed to precipitation over time. The stability of these conjugates was also investigated in PBS/10% DMSO pH 7.4 and in human plasma by LC-MS analysis to show the same precipitation behavior (Figure S7 and S9, Supporting Information). In addition to this, four oxidized species of **Ru-Acryl-BBN** were identified (Figure S8 and S10, Supporting Information), in which the oxidation of the *C*-terminal methionine (Met) into a sulfoxide was detected by LC-MS/MS analysis (Table S1, Supporting Information). The transformation of the native Met thioether into a polar sulfoxide in BBN peptide is expected to substantially reduce its binding affinity and, consequently, the biological activity of BBN constructs, as previously reported by Walsh and co-workers.[19] Therefore, it is highly recommended to prevent extended light exposure of these constructs before any biological evaluation as the incorporated Ru(II) complex is an efficient photosensitizer.

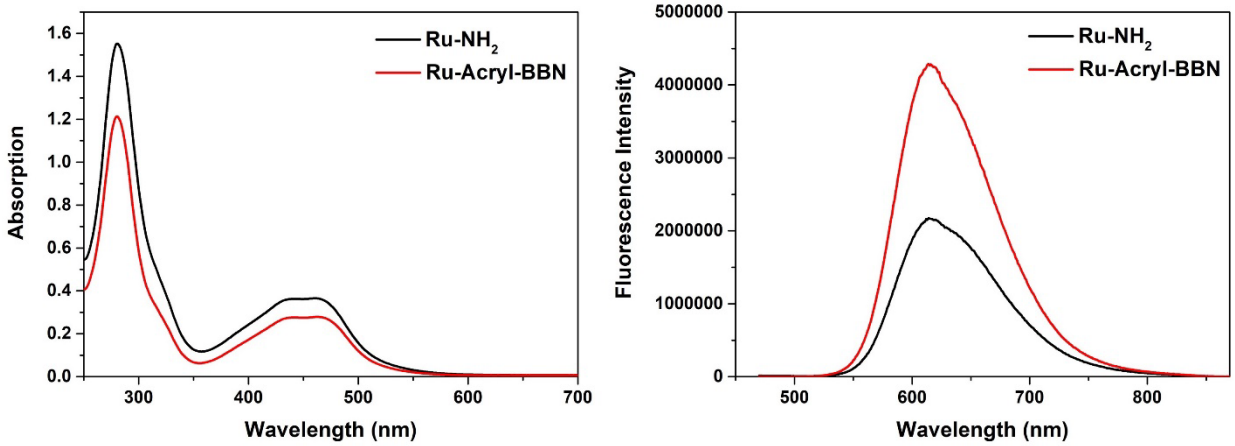

Figure 2. Absorption (left) and fluorescence (right) spectra of **Ru-Acryl-BBN** (red line) and **Ru-NH₂** (black line). The spectra were recorded in water at a concentration of 50 μM).

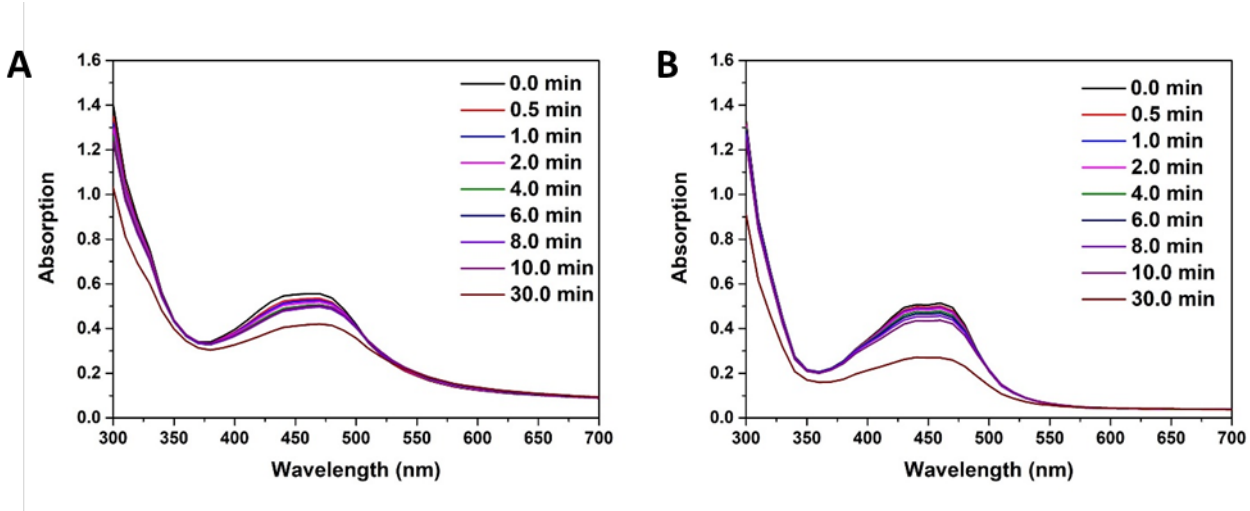

Figure 3. **Ru-NH₂** (50 μM) absorption spectrum changes upon irradiation (510 nm, 4.33 mW/cm^2) (**A**: PBS; **B**: Acetonitrile).

Then, the biological activities of both BBN conjugates and the precursor complex **Ru-NH$_2$** were evaluated in HT-29 colorectal, PC-3 prostate human adenocarcinoma cells and mouse colon carcinoma cells CT-26. The phototoxicity of these compounds was assessed under standardized procedures with 4 h incubation prior to irradiation at 595 nm for 2 h (light dose 22.47 J/cm^2). Dark controls, in which the cells are treated identically but without light irradiation were also acquired. The cell viability was evaluated 44 h later using a resazurin fluorimetric assay. The active metabolite of the clinically approved PDT agent 5-aminolaevulinic acid,[20] protoporphyrin IX (Pp IX) was used as a positive control. Worthy of note, the light exposure alone did not affect the viability of the tested cells. As shown in Table 1, upon light irradiation, both **Ru-Acryl-BBN** and **Ru-Mal-BBN** conjugates presented similarly high toxicity levels within the low micromolar range as the **Ru-NH$_2$** compound. In contrast, dark controls of the conjugates showed no toxicity at up to 100 μM, whereas **Ru-NH$_2$** maintained low IC$_{50}$ levels, contributing to an overall improvement of the photoindex (PI), with the exception of HT-29 cells. Due to the comparable phototoxicity profile of both conjugates, the following experiments were performed with **Ru-Acryl-BBN**.

Table 1. IC$_{50}$ values for **Ru-NH$_2$** complex, **Ru-Acryl-BBN** and **Ru-Mal-BBN** conjugates and Pp IX obtained in dark controls and upon irradiation at 595 nm for 2 h (light dose 22.47 J/cm^2).

IC$_{50}$ (μM)	**Ru-NH$_2$**			**Ru-Acryl-BBN**			**Ru-Mal-BBN**			**Pp IX**		
Cell line	dark	light	PI	dark	light	(PI	dark	light	PI	dark	light	PI
PC-3	18±2	1.6±0.2	11	>100	4.8±0.3	>21	>100	3.2±0.5	>31	1.4±0.1	0.3±0.1	5
HT-29	>100	4±2	>25	>100	8±1	>13	>100	8±3	>13	94±5	0.6±0.5	157
CT26	8±0.6	0.5±0.1	16	>100	0.6±0.04	>167	>100	18±0.2	>6	2.6±0.3	0.3±0.1	9

Note: The C$_0$ controls in dark and light showed that light exposure did not affect the cell viability. PI = IC$_{50}$ dark / IC$_{50}$ light. .Data are presented as means ± standard deviation (SD) of three independent replicates.

Next, in order to evaluate the expression profile of GRPR at the surface of the tested cells, an in-cell ELISA assay was performed. In agreement to previous reports, the PC-3 cell line expresses high levels of GRPR,[21] followed by HT-29 and CT26 cells, according to the measurements illustrated in Figure 4.

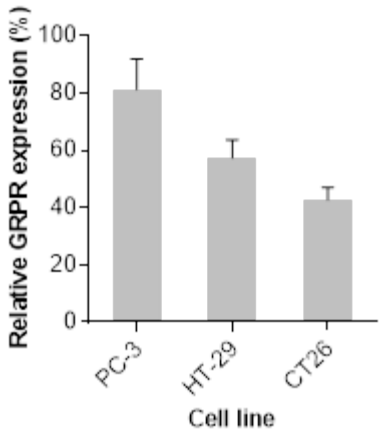

Figure 4. Relative quantification of GRPR expression levels by in-cell indirect ELISA with a rabbit anti-GRPR antibody and a secondary HRP-conjugated anti-rabbit IgG antibody. Data are presented as means ± standard deviation (SD) of eight independent replicates.

To further elucidate on the internalization process of **Ru-Acryl-BBN** and **Ru-NH_2**, a time-dependent cellular uptake was performed in PC-3 cell line owing to the observed overexpression of GRPR. The cellular uptake of these compounds was measured by ICP-MS analysis of cells incubated with the complexes for an increasing amount of time. As illustrated in Figure 5A, the two compounds have different uptake profiles over time. The **Ru-Acryl-BBN** displayed a fast internalization equilibrium that is established after about 1 h of incubation, which is in accordance with the time frame for the expected maximum GRPR-mediated internalization at 37ºC.[22] On the other hand, **Ru-NH_2** presented an exponential increase of Ru uptake over time, affording an up to 10-fold increased uptake of ruthenium after 4 h compared to the conjugated to BBN peptide. Then, the cellular uptake of these compounds was measured after 4 h of incubation on the three cancer cell lines (Figure 5B). Overall, the **Ru-NH_2** complex accumulates in higher amounts in all tested cell lines in comparison to **Ru-Acryl-BBN**. Altogether, these results suggest different internalization mechanisms for the two compounds, probably due to the large size and bulkiness of the bioconjugate **Ru-Acryl-BBN** that hinder its passive diffusion through the cell membrane. Additionally, it is expected that the appended BBN peptide mediates the internalization through GRPR recognition. Surprisingly, these quantitative studies on PC-3 cells suggest that there is no direct correlation between the internalization efficiency of **Ru-Acryl-BBN** and the GRPR expression level. We expected to observe a higher Ru uptake in the prostate cancer cells in comparison to the other tested cell lines. Nevertheless, this poor correlation might be due to the denoted fast oxidation of the *C*-terminal methionine to sulfoxide derivative of **Ru-Acryl-BBN**, which might prevent the receptor recognition and decrease the binding affinity of the

conjugate to GRPRs.

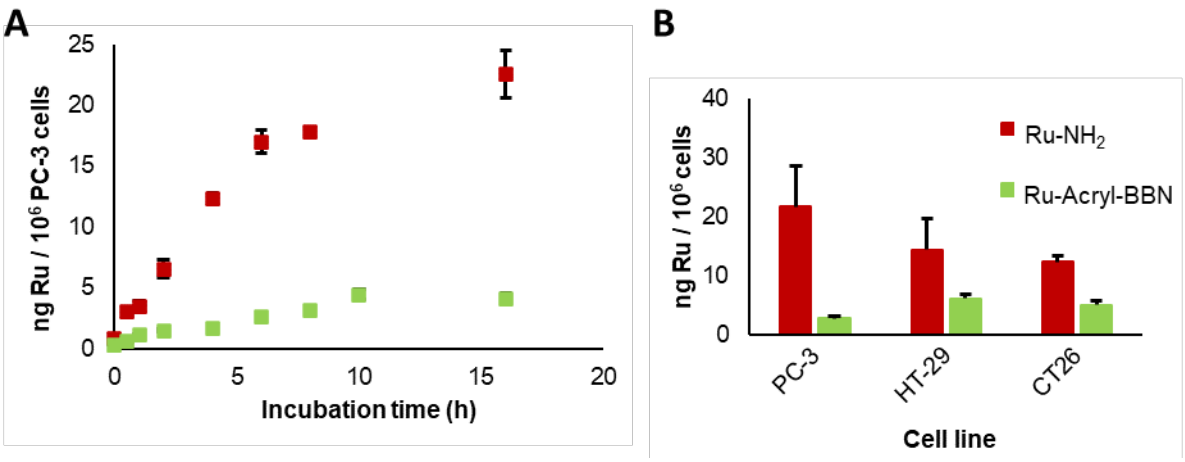

Figure 5. Cellular uptake measurements of **Ru-NH₂** (red) and **Ru-Acryl-BBN** (green) based on ICP-MS analysis of digested cells. A) Time-dependent cellular uptake of ruthenium in PC-3 cells over 16 h of incubation time. B) Ruthenium cellular uptake on PC-3, HT-29 and CT26 cancer cells after 4 h incubation. Results are presented as a mean ± SD of two (A) and three (B) replicates.

On the other hand, mouse colon carcinoma CT26 cells showed to be particularly sensitive to **Ru-Acryl-BBN**, with IC_{50} values in the nanomolar range after irradiation and no toxicity in the dark. Intrigued by these results, the subcellular localization of **Ru-NH₂** and **Ru-Acryl-BBN** in these cells was investigated by confocal laser microscopy leveraging the intrinsic luminescence of the Ru(II) compounds. As shown in Figure 6, both **Ru-NH₂** and **Ru-Acryl-BBN** could penetrate into CT26 cells and accumulate in membrane-bound organelles or vesicles, as suggested by the observed punctate pattern. In colocalization experiments, no overlap was observed with a mitochondrial dye, while a partial overlap could be observed with a lysosomal dye, suggesting that **Ru-NH₂** and **Ru-Acryl-BBN** can accumulate in lysosomes but not in mitochondria. As regards to **Ru-Acryl-BBN** conjugate, it is expected to undergo GRPR-mediated endocytosis promoting intrinsic accumulation in intracellular vesicles like lysosomes, as previously demonstrated.[22a, 22b] **Ru-NH₂** lysosomal accumulation might be due to a nano-aggregation behavior as was suggested in a recent study.[23] In fact, dynamic light scattering data measured in 10% FBS in PBS showed a very large polydispersity index **Ru-NH₂**, where as **Ru-Acryl-BBN** compares well with the control (Figure 7). Following dilution in culture medium, **Ru-NH₂** and other structurally similar complexes show an aggregation behavior leading to the formation of positively charged nanoparticles. This phenomenon promotes their internalization through endocytosis, and thus their accumulation in lysosomes.[23] Indeed, lysosome-targeted PSs are known to be particularly effective,[24] therefore the lysosomal accumulation of both complexes leads to a similar PDT efficiency. On the other hand, as previously showed in Figure 5B, the higher uptake of **Ru-NH₂** in these cells result in higher toxicity for this compound in the dark.

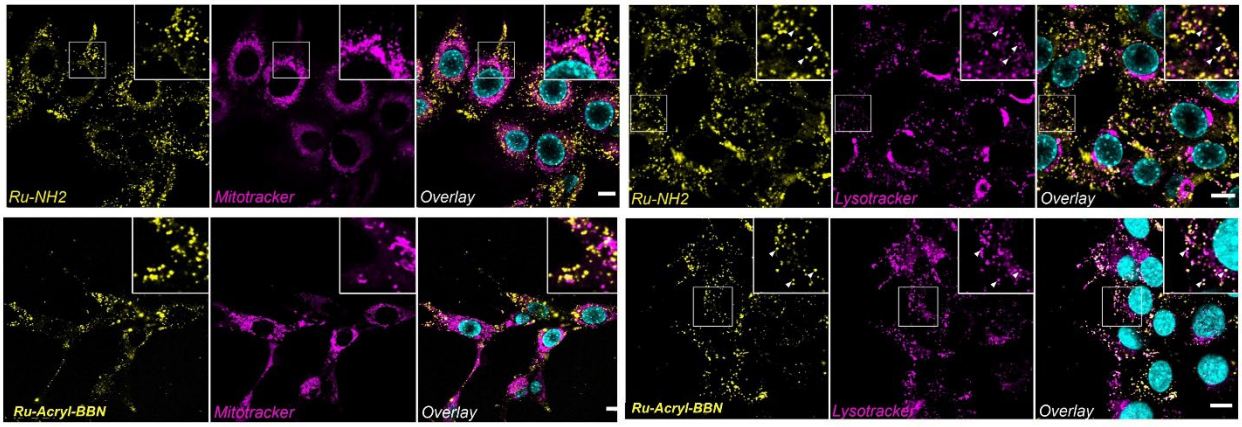

Figure 6. Confocal imaging in CT26 cell line after 4 h incubation with 5 μM of **Ru-NH$_2$** complex or **Ru-Acryl-BBN** (yellow). Mitotracker or Lysotracker (magenta) and Hoechst 33342 (cyan) were added for co-localization studies with mitochondria or lysosomes and cell nuclei respectively. Arrowheads indicate colocalization between **Ru-NH$_2$** or **Ru-Acryl-BBN** and Lysotracker. All scale bars: 10 μm.

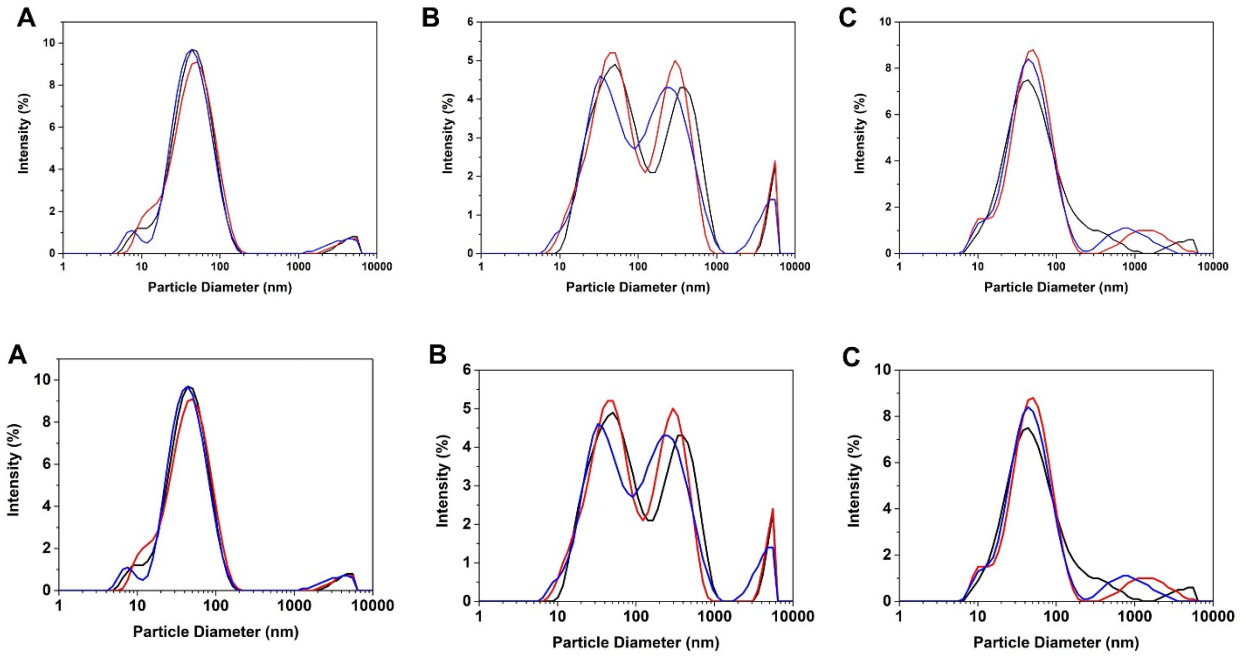

	A	B	C
Polydispersity index	0.34±0.01	0.71±0.05	0.38±0.01

Figure 7. DLS data: particle size distribution by the intensity of Ru-NH$_2$ (20 μM) and Ru-Acryl-BBN (20 μM) in 10% FBS in PBS. (A) Control: Only PBS with 10% FBS ; (B) Ru-NH$_2$ in PBS with 10% FBS; (C) Ru-Acryl-BBN in PBS with 10% FBS. The three curves represent three measurements of the same sample. The table indicates the polydispersity indexes of the corresponding nanoparticles.

Conclusions

The straightforward and easy to handle NHS-activated acrylamide conjugation strategy was efficiently applied on the bioconjugation of a Ru(II) polypyridyl complex bearing a nucleophilic

amine to a Cys-Bombesin peptide to synthesize the **Ru-Acryl-BBN** conjugate. This highlights the versatility of this approach for irreversible *N*-terminal Cys functionalization, which competes with conventional maleimide chemistry. Preliminary photophysical and LC-MS studies revealed a partial precipitation in physiological-like media of both **Ru-NH_2** and **Ru-Acryl-BBN** and the oxidation of the *C*-terminal Met of **Ru-Acryl-BBN**, which is a key side chain residue for GRPR recognition. Nevertheless, the afforded BBN bioconjugates out-performed the **Ru-NH_2** complex in therapeutic PDT efficiency, as the insertion of the BBN peptide was shown to be beneficial in decreasing the toxicity of the corresponding conjugate in the dark. Gratifyingly, these conjugates exhibited IC_{50} values within the same low micromolar range following irradiation in comparison to the **Ru-NH_2** complex. This results in an overall improvement of the observed PI and further indicates that, even though the cellular uptake is not as efficient as for the **Ru-NH_2** complex, the phototoxicity is maintained. Confocal imaging studies on CT-26 cancer cell line corroborated the high uptake of both Ru(II) complexes and their accumulation in intracellular vesicles like lysosomes. It is hypothesized that the lysosomal content on Ru(II) complex is the major contributor for the observed PDT effect. This confirms that the subcellular localization of the PS is much more important than its overall intracellular concentration. In summary, the bioconjugation of Ru(II) complexes to peptides is a promising strategy to improve their PDT efficiency. It might also help to selectively accumulate the complexes in cancer cells, although this did not seem to be the case with our BBN-conjugated PS. Importantly, this work also shows that one should be cautious in the choice of the targeting peptide when designing peptide-targeted PSs. This peptide should not contain any oxidizable residues that are essential to its affinity for its target.

Experimental Section

A full description of methods and data that support the results reported herein are provided in the Supporting Information.

Synthesis of $[Ru(bphen)_2dmbipyNH_2](PF_6)_2$

A mixture of $Ru(bphen)_2Cl_2$ (300 mg, 0.359 mmol, 1.0 equiv) and $dmbipyNH_2$ ligand (86 mg, 0.43 mmol, 1.2 equiv) dissolved in EtOH (38 mL) was refluxed for 6 h. After cooling to room temperature, a saturated solution of NH_4PF_6 was added. The suspension was stored at 4 ºC overnight. The solid was filtered and washed with water, EtOH and Et_2O. The compound was purified by column chromatography on silica gel with an CH_3CN /aq. KNO_3 (0.4 M) solution (10:1), Rf = 0.46). The collected fractions were combined, evaporated and dissolved in DCM to remove excess of KNO_3. The solution was filtered, evaporated and the residue was dissolved in EtOH.

NH_4PF_6 sat. solution was added and the mixture was stored at 4 ºC overnight. The solid was filtered, washed with water, EtOH and Et_2O and eluted from the filter with DCM. The solvent was removed and the residue dried under high vacuum for 72 h to obtain pure product **[Ru(bphen)$_2$dmbipyNH$_2$](PF$_6$)$_2$** (106 mg, 0.110 mmol, 31% yield) as a red crystalline solid. **^{1}H NMR** (400 MHz, Acetonitrile-d_3) δ 8.55 (s, 1H), 8.43 (s, 1H), 8.30 (d, *J* = 5.4 Hz, 1H), 8.28 – 8.24 (m, 1H), 8.24 – 8.15 (m, 4H), 8.10 (dd, *J* = 9.4, 5.5 Hz, 2H), 7.89 (d, *J* = 5.8 Hz, 1H), 7.77 (dd, *J* = 5.5, 1.5 Hz, 2H), 7.71 (d, *J* = 5.8 Hz, 1H), 7.69 – 7.55 (m, 22H), 7.35 (d, *J* = 5.9 Hz, 1H), 7.26 (dd, *J* = 5.7, 0.9 Hz, 1H), 4.31 (s, 1H), 2.58 (s, 3H). **^{13}C NMR** (100 MHz, CD_3CN) δ 158.4, 156.6, 152.9, 152.6, 152.4, 152.3, 151.8, 151.3, 149.5, 149.41, 149.38, 148.9, 148.7, 148.6, 142.9, 136.25, 136.19, 130.3, 130.2, 130.05, 129.99, 129.6, 129.5, 129.4, 129.4, 129.3, 127.4, 126.8, 126.7, 126.6, 126.4, 125.6, 124.5, 42.8, 20.8. **ESI$^+$-HRMS** calcd for $C_{60}H_{45}N_7Ru$ $[M]^{2+}$: 482.6384, found 482.6380. Elemental analysis calcd for $C_{60}H_{45}F_{12}N_7P_2Ru.HPF_6$ (%): C 51.44, H 3.31, N 7.00; found: C 50.90, H 3.74, N 7.13.

Synthesis of [Ru NHS-activated acrylamide](PF$_6$)$_2$

In a 5 mL round bottom flask di-NHS activated fumarate (23.2 mg, 75 µmol, 1.6 equiv) was suspended in CH_3CN (4.8 mL). Then, a solution of **[Ru(bphen)$_2$dmbipyNH$_2$](PF$_6$)$_2$** (47 mg, 48 µmol, 1.0 equiv) in CH_3CN (4.8 mL) with triethylamine (40 µL, 0.29 mmol, 6.0 equiv) was added dropwise to the reaction mixture which was stirred at r.t. shaded from light. The reaction was stirred for 1 h until complete consumption of the amine, as confirmed by silica TLC (CH_3CN/aq. KNO_3 (0.4 M) solution (10:1), Rf = 0.46 for amine starting material and Rf = 0.63 for amidation product). The solvent was removed under vacuum and the resulting solid was dissolved in a minimum amount of CH_3CN and H_2O (5 mL) was added to form an orange red precipitate. The suspension was centrifuged and the precipitate washed with H_2O (5 mL) and twice with Et_2O (5 mL). The red solid obtained by centrifugation was dried under high vacuum to afford pure product **Ru NHS-activated acrylamide** (48 mg, 0.033 mmol, 69% yield) as a red crystalline solid. **^{1}H NMR** (500 MHz, Acetonitrile-d_3) δ 8.52 (s, 1H), 8.49 (s, 1H), 8.32 (t, *J* = 5.5 Hz, 3H), 8.26 – 8.17 (m, 5H), 8.13 (q, *J* = 6.5, 6.0 Hz, 2H), 7.79 (d, *J* = 4.8 Hz, 4H), 7.75 – 7.51 (m, 30H), 7.34 (d, *J* = 15.6 Hz, 1H), 7.27 (dt, *J* = 21.1, 5.0 Hz, 2H), 6.91 (dd, *J* = 15.3, 5.8 Hz, 1H), 4.68 (d, *J* = 6.0 Hz, 1H), 2.81 (s, 3H), 2.58 (s, 4H). **^{13}C NMR** (126 MHz, CD_3CN) δ 170.9, 164.0, 162.2, 158.4, 157.6, 153.2, 153.13, 153.06, 152.8, 152.3, 151.6, 151.4, 150.04, 150.00, 149.9, 149.6, 149.5, 149.39, 149.36, 142.1, 136.8, 136.7, 130.9, 130.8, 130.7, 130.6, 130.2, 130.1, 130.0, 129.97, 129.95, 129.4, 127.2, 127.0, 126.6, 126.2, 124.6, 123.1, 123.1, 43.0, 26.4, 21.3. **ESI$^+$-HRMS** calcd for $C_{68}H_{50}N_8O_5Ru$ $[M]^{2+}$: 580.1468, found 580.1456.

Synthesis of [Ru-Maleimide]$(PF_6)_2$

[Ru(bphen)$_2$dmbipyNH$_2$]$(PF_6)_2$ (50 mg, 0.04 mmol, 1.0 equiv) and maleic anhydride (38 mg, 0.39 mmol, 10.0 equiv) were suspended in acetic acid (10 mL) and refluxed for 10 h under N_2 atmosphere. The solvent was evaporated and the residue dissolved in 10 mL of H_2O. A saturated, aq. NH_4PF_6 solution was added and the resulting precipitate was collected by vacuum filtration. The solid was washed with H_2O (50 mL) and Et_2O (50 mL). The product was purified by column chromatography on silica gel with an CH_3CN /aq. KNO_3 (0.4 M) solution (10:1), Rf = 0.53. The fractions containing the product were united and the solvent was removed. The residue was dissolved in CH_3CN and undissolved KNO_3 was removed by filtration. The solvent was evaporated and the product was dissolved in H_2O (20 mL). Upon addition of NH_4PF_6 the product precipitated as a PF_6 salt. The solid was obtained by filtration and was washed with H_2O (50 mL) and Et_2O (50 mL). The product **[Ru-Maleimide]$(PF_6)_2$** was dried in high vacuum. Yield: 71%. **^{1}H NMR** (400 MHz, CD_3CN) δ = 8.65 (s, 1H), 8.57 (s, 1H), 8.32 (1H, d, *J* = 5.5 Hz), 8.29 (1H, d, *J* = 5.5 Hz), 8.21-8.15 (m, 6H), 8.11 (1H, d, *J* = 5.5 Hz), 7.79-7.75 (m, 3H), 7.69-7.56 (m, 22H), 7.23 (2H, dd, *J* = 5.8, 1.4 Hz), 6.90 (s, 2H), 4.84 (s, 2H), 2.57 (s, 3H); **^{13}C NMR** (100 MHz, CD_3CN) δ = 171.6, 158.5, 157.2, 153.0, 153.0, 152.9, 152.2, 151.5, 149.9, 149.9, 149.8, 149.4, 149.3, 149.2, 149.2, 149.1, 136.7, 136.6, 135.7, 130.7, 130.6, 130.5, 130.5, 130.0, 130.0, 129.8, 129.4, 127.1, 127.0, 126.9, 126.5, 126.2, 123.0, 40.6, 21.1; **ESI$^+$-HRMS** calcd for $C_{64}H_{45}N_7O_2Ru$ *m/z* $[M]^{2+}$ 522.6334; found: 522.6347.

Cys-Bombesin functionalization with Ru complexes

A fresh solution of Cys-Bombesin (Cys-BBN$_{7-14}$) in 2 mL of ammonium acetate 20 mM, pH 7.0 (5.22 mg, 5.00 µmol, 2.50 mM) was prepared and diluted in a mixture of ammonium acetate 20 mM, pH 7 and ACN (1:1) (6 mL). Then, a solution of **Ru NHS-activated acrylamide** or **Ru-Mal** (6.00 µmol, 1.2 equiv) in ACN (2 mL) was immediatly added to the mixture. The reaction was agitated at r.t. shaded from light. After for 10 min, the crude mixtures were purified by preparative HPLC. **Ru-Acryl-BBN** was collected at RT 19.4 min and 19.9 min with isolated yields ranging 20-74%, while **Ru-Mal-BBN** was collected at RT 19.4 min with isolated yields 15-70%.

Each collected fraction was analysed by ESI$^+$-HRMS before and after freeze-drying to check the presence of oxidized species. The samples presenting higher amounts of those undesired species were discarded. Finally all samples were combined, freeze-dried again and the final purity was verified by HPLC and ESI$^+$-HRMS.

Conflicts of interest

The authors declare no competing financial interests.

Acknowledgments

The authors acknowledge the financial support from Fundação para a Ciência e a Tecnologia, Ministério da Ciência e da Tecnologia, Portugal (SFRH/BD/132710/2017. Research Institute for Medicines (iMed.ULisboa) acknowledges the financial support of Fundação para a Ciência e Tecnologia (Projects: PTDC/QUI-OUT/3989/2021; UIDB/04138/2020 and UIDP/04138/2020). The NMR spectrometers are part of the National NMR Network (PTNMR) and are partially supported by Infrastructure Project Nº 022161 (co-financed by FEDER through COMPETE 2020, POCI and PORL and FCT through PIDDAC).. Y. W. thanks the China Scholarship Council for financial funding. E.D.J. thanks to the University of Castilla-La Mancha for the financial funding. This work was also financially supported by an ERC Consolidator Grant PhotoMedMet to G.G. (GA 681679), has received support under the program “Investissements d’Avenir” launched by the French Government and implemented by the ANR with the reference ANR-10-IDEX-0001-02 PSL (G.G.). Part of the ICP-MS measurements was supported by IPGP multidisciplinary program PARI, and by Paris–IdF region SESAME Grant no. 12015908.

Keywords: Bombesin; Medicinal Inorganic Chemistry; Metals in Medicine; Photodynamic Therapy; Ruthenium.

References

[1] F. Wei, T. W. Rees, X. Liao, L. Ji, H. Chao, *Coord. Chem. Rev.* **2021**, *432*, 213714.

[2] a) J. Liu, C. Zhang, T. W. Rees, L. Ke, L. Ji, H. Chao, *Coord. Chem. Rev.* **2018**, *363*, 17; b) V. Novohradsky, A. Zamora, A. Gandioso, V. Brabec, J. Ruiz, V. Marchán, *Chem. Commun.* **2017**, *53*, 5523; c) S. Monro, K. L. Colón, H. Yin, J. Roque, III, P. Konda, S. Gujar, R. P. Thummel, L. Lilge, C. G. Cameron, S. A. McFarland, *Chem. Rev.* **2019**, *119*, 797.

[3] a) U. Ndagi, N. Mhlongo, M. E. Soliman, *Drug Des., Dev. Ther.* **2017**, *11*, 599; b) E. J. Anthony, E. M. Bolitho, H. E. Bridgewater, O. W. L. Carter, J. M. Donnelly, C. Imberti, E. C. Lant, F. Lermyte, R. J. Needham, M. Palau, P. J. Sadler, H. Shi, F. X. Wang, W. Y. Zhang, Z. Zhang, *Chem. Sci.* **2020**, *11*, 12888; c) E. Boros, P. J. Dyson, G. Gasser, *Chem* **2020**, *6*, 41; d) A. Johnson, J. Northcote-Smith, K. Suntharalingam, *Trends Chem.* **2021**, *3*, 47; e) J. Karges, *ChemBioChem* **2020**, *21*, 3044.

[4] a) J. Karges, *Angew. Chem. Int. Ed.* **2022**, *61*, e202112236; b) S. A. McFarland, A. Mandel, R. Dumoulin-White, G. Gasser, *Curr. Opin. Chem. Biol.* **2020**, *56*, 23.

[5] a) F. Heinemann, J. Karges, G. Gasser, *Acc. Chem. Res.* **2017**, *50*, 2727; b) C. Mari, V. Pierroz, S. Ferrari, G. Gasser, *Chem. Sci.* **2015**, *6*, 2660; c) L. Zeng, P. Gupta, Y. Chen,

E. Wang, L. Ji, H. Chao, Z.-S. Chen, *Chem. Soc. Rev.* **2017**, *46*, 5771; d) J. D. Knoll, C. Turro, *Coord. Chem. Rev.* **2015**, *282-283*, 110; e) J. Roque Iii, D. Havrylyuk, P. C. Barrett, T. Sainuddin, J. McCain, K. Colón, W. T. Sparks, E. Bradner, S. Monro, D. Heidary, C. G. Cameron, E. C. Glazer, S. A. McFarland, *Photochem. Photobiol.* **2020**, *96*, 327; f) H. D. Cole, J. A. Roque Iii, L. M. Lifshits, R. Hodges, P. C. Barrett, D. Havrylyuk, D. Heidary, E. Ramasamy, C. G. Cameron, E. C. Glazer, S. A. McFarland, *Photochem. Photobiol.* **2022**, *98*, 73; g) P. Konda, J. A. Roque Iii, L. M. Lifshits, A. Alcos, E. Azzam, G. Shi, C. G. Cameron, S. A. McFarland, S. Gujar, *Am. J. Cancer Res.* **2022**, *12*, 210; h) A. Chettri, H. D. Cole, J. A. Roque Iii, K. R. A. Schneider, T. Yang, C. G. Cameron, S. A. McFarland, B. Dietzek-Ivanšić, *J. Phys. Chem. A* **2022**, *126*, 1336; i) O. E. Oladipupo, S. R. Brown, R. W. Lamb, J. L. Gray, C. G. Cameron, A. R. DeRegnaucourt, N. A. Ward, J. F. Hall, Y. Xu, C. M. Petersen, F. Qu, A. B. Shrestha, M. K. Thompson, M. Bonizzoni, C. E. Webster, S. A. McFarland, Y. Kim, E. T. Papish, *Photochem. Photobiol.* **2022**, *98*, 102; j) L. M. Lifshits, J. A. Roque Iii, P. Konda, S. Monro, H. D. Cole, D. von Dohlen, S. Kim, G. Deep, R. P. Thummel, C. G. Cameron, S. Gujar, S. A. McFarland, *Chem. Sci.* **2020**, *11*, 11740; k) G. Ghosh, H. Yin, S. M. A. Monro, T. Sainuddin, L. Lapoot, A. Greer, S. A. McFarland, *Photochem. Photobiol.* **2020**, *96*, 349; l) G. Ghosh, K. L. Colón, A. Fuller, T. Sainuddin, E. Bradner, J. McCain, S. M. A. Monro, H. Yin, M. W. Hetu, C. G. Cameron, S. A. McFarland, *Inorg. Chem.* **2018**, *57*, 7694; m) V. Ramu, S. Aute, N. Taye, R. Guha, M. G. Walker, D. Mogare, A. Parulekar, J. A. Thomas, S. Chattopadhyay, A. Das, *Dalton Trans.* **2017**, *46*, 6634.

[6] J. Karges, F. Heinemann, M. Jakubaszek, F. Maschietto, C. Subecz, M. Dotou, R. Vinck, O. Blacque, M. Tharaud, B. Goud, E. Viñuelas Zahínos, B. Spingler, I. Ciofini, G. Gasser, *J. Am. Chem. Soc.* **2020**, *142*, 6578.

[7] a) L. B. Josefsen, R. W. Boyle, *Br. J. Pharmacol.* **2008**, *154*, 1; b) M. Martínez-Alonso, G. Gasser, *Coord. Chem. Rev.* **2021**, *434*, 213736; c) K. S. Gkika, D. Cullinane, T. E. Keyes, *Top. Curr. Chem.* **2022**, *380*, 30; d) L. Holden, C. S. Burke, D. Cullinane, T. E. Keyes, *RSC Chem. Biol.* **2021**, *2*, 1021; e) A. Gandioso, A. Rovira, H. Shi, P. J. Sadler, V. Marchán, *Dalton Trans.* **2020**, *49*, 11828; f) A. Gandioso, E. Shaili, A. Massaguer, G. Artigas, A. González-Cantó, J. A. Woods, P. J. Sadler, V. Marchán, *Chem. Commun.* **2015**, *51*, 9169; g) L. Ke, F. Wei, L. Xie, J. Karges, Y. Chen, L. Ji, H. Chao, *Angew. Chem. Int. Ed.* **2022**, *61*, e202205429; h) J. Bonelli, E. Ortega-Forte, G. Vigueras, M. Bosch, N. Cutillas, J. Rocas, J. Ruiz, V. Marchán, *Inorg. Chem. Front.* **2022**, *9*, 2123; i) J. Li, L. Zeng, Z. Wang, H. Chen, S. Fang, J. Wang, C.-Y. Cai, E. Xing, X. Liao, Z.-W. Li, C. R. Ashby Jr, Z.-S. Chen, H. Chao, Y. Pan, *Adv. Mater.* **2022**, *34*, 2100245; j) M. R. Gill, J. U. Menon, P. J. Jarman, J. Owen, I. Skaripa-Koukelli, S. Able, J. A. Thomas, R. Carlisle, K. A. Vallis, *Nanoscale* **2018**, *10*, 10596.

[8] P. Moreno, I. Ramos-Álvarez, T. W. Moody, R. T. Jensen, *Expert Opin. Ther. Targets* **2016**, *20*, 1055.

[9] a) I. Ramos-Álvarez, P. Moreno, S. A. Mantey, T. Nakamura, B. Nuche-Berenguer, T. W. Moody, D. H. Coy, R. T. Jensen, *Peptides* **2015**, *72*, 128; b) R. T. Jensen, J. F. Battey, E. R. Spindel, R. V. Benya, *Pharmacol. Rev.* **2008**, *60*, 1.

[10] D. B. Cornelio, R. Roesler, G. Schwartsmann, *Ann. Oncol.* **2007**, *18*, 1457.

[11] K. Szepeshazi, A. V. Schally, A. Nagy, G. Halmos, *Pancreas* **2005**, *31*.

[12] A. A. Begum, P. M. Moyle, I. Toth, *Bioorg. Med. Chem.* **2016**, *24*, 5834.

[13] L. Ma, P. Yu, B. Veerendra, T. L. Rold, L. Retzloff, A. Prasanphanich, G. Sieckman, T. J. Hoffman, W. A. Volkert, C. J. Smith, *Mol. Imaging* **2007**, *6*, 171.

[14] a) K. Kim, H. Zhang, S. La Rosa, S. Jebiwott, P. Desai, S. Kimm, A. Scherz, J. A. O'Donoghue, W. A. Weber, J. A. Coleman, *Clin. Cancer Res.* **2017**, *23*, 3343; b) C. Mari, V. Pierroz, A. Leonidova, S. Ferrari, G. Gasser, *Eur. J. Inorg. Chem.* **2015**, *2015*, 3879; c)

A. Leonidova, V. Pierroz, R. Rubbiani, J. Heier, S. Ferrari, G. Gasser, *Dalton Trans.* **2014**, *43*, 4287.
[15] M. J. S. A. Silva, H. Faustino, J. A. S. Coelho, M. V. Pinto, A. Fernandes, I. Compañón, F. Corzana, G. Gasser, P. M. P. Gois, *Angew. Chem. Int. Ed.* **2021**, *60*, 10850.
[16] I. Bratsos, Alessio, E., Ringenberg, M. E., Ruthenium Complexes in *Inorg. Synth., Vol. 35* (Ed.: T. B. Rauchfuss), Wiley-Blackwell, **2010**, 148.
[17] A. Notaro, M. Jakubaszek, N. Rotthowe, F. Maschietto, R. Vinck, P. S. Felder, B. Goud, M. Tharaud, I. Ciofini, F. Bedioui, R. F. Winter, G. Gasser, *J. Am. Chem. Soc.* **2020**, *142*, 6066.
[18] M. L. Bennasar, E. Zulaica, D. Solé, S. Alonso, *Tetrahedron* **2012**, *68*, 4641.
[19] S. R. Vigna, A. S. Giraud, J. R. Reeve, J. H. Walsh, *Peptides* **1988**, *9*, 923.
[20] A. Casas, *Cancer Lett.* **2020**, *490*, 165.
[21] a) C. Dubuc, R. Langlois, F. Bénard, N. Cauchon, K. Klarskov, P. Tone, J. E. van Lier, *Bioorg. Med. Chem. Lett.* **2008**, *18*, 2424; b) X. Li, H. Cai, X. Wu, L. Li, H. Wu, R. Tian, *Front. Chem.* **2020**, *8*, 583309; c) A. Stangelberger, A. V. Schally, M. Letsch, K. Szepeshazi, A. Nagy, G. Halmos, C. A. Kanashiro, E. Corey, R. Vessella, *Int. J. Cancer* **2006**, *118*, 222.
[22] a) E. F. Grady, L. W. Slice, W. O. Brant, J. H. Walsh, D. G. Payan, N. W. Bunnett, *J. Biol. Chem.* **1995**, *270*, 4603; b) J. A. Lunn, H. Wong, E. Rozengurt, J. H. Walsh, *Am. J. Physiol. Cell Physiol.* **2000**, *279*, C2019; c) M. Schumann, T. Nakagawa, S. A. Mantey, K. Tokita, D. J. Venzon, S. J. Hocart, R. V. Benya, R. T. Jensen, *J. Pharmacol. Exp. Ther.* **2003**, *307*, 597.
[23] R. Vinck, A. Gandioso, P. Burckel, B. Saubaméa, K. Cariou, G. Gasser, *Inorg. Chem.* **2022**, *61*, 13576.
[24] R. Wang, X. Li, J. Yoon, *ACS Appl. Mater.* **2021**, *13*, 19543.

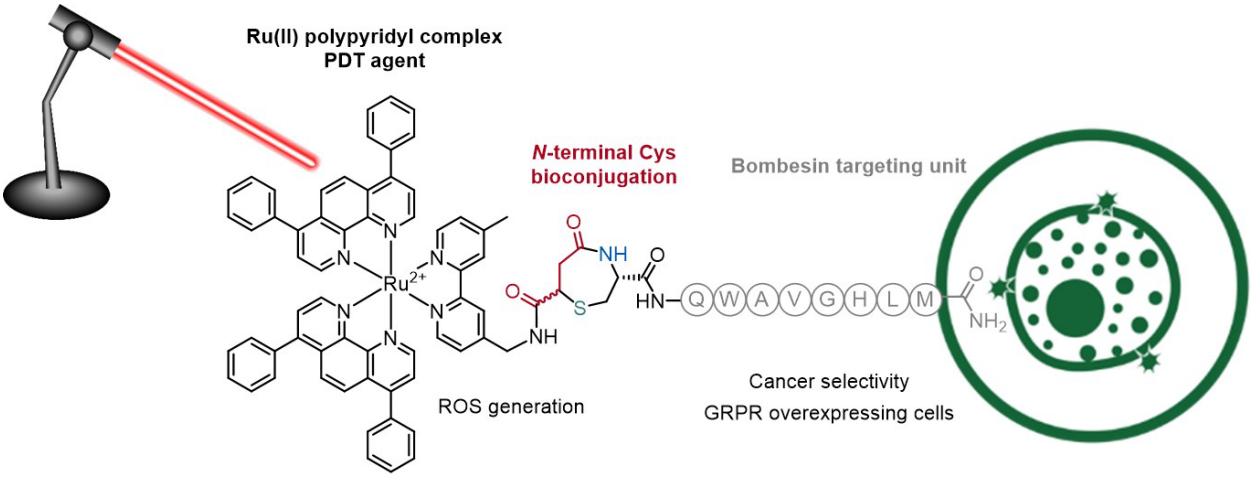

Decreasing the off-target and general cytotoxicity in the dark of new potential photosensitizers are relevant factors for increased photodynamic therapy (PDT) efficiency. In this article, we explored the site-selective bioconjugation of a promising Ru(II) polypyridyl complex to the *N*-terminal Cys modified bombesin peptide for improved PDT towards cancer cells.